

Advance Publication

## Experimental Animals

Received: 2023.2.5

Accepted: 2023.6.29

J-STAGE Advance Published Date: 2023.7.6

1 **Model animals**  
2 **Humanized CD36 mouse model supports the preclinical evaluation of**  
3 **therapeutic candidates targeting CD36**

4 Xiulong Xie<sup>a,b,c,#</sup>, Zhenlan Niu<sup>c,#</sup>, Linlin Wang<sup>c,#</sup>, Xiaofei Zhou<sup>c</sup>, Xingyan Yu<sup>a,b,c</sup>,  
5 Hongyan Jing<sup>a,b,c</sup>, Yi Yang<sup>a,b,c,1,\*</sup>

6 *<sup>a</sup>Jiangxi University of Traditional Chinese Medicine, Nanchang, Jiangxi,*  
7 *330004, China*

8 *<sup>b</sup>Yangtze Delta Drug Advanced Research Institute, Haimen, Jiangsu, 226133, China*

9 *<sup>c</sup>Biocytogen Pharmaceuticals (Beijing), Beijing 102600, China*

10  
11  
12  
13  
14  
15  
16  
17  
18  
19  
20  
21

---

# : These authors contributed equally to this work.

\* **Corresponding authors:** Beijing, [benny.yang@bbctg.com.cn](mailto:benny.yang@bbctg.com.cn).

Supplementary Figure: refer to J-STAGE

22 **Abstract**

23 CD36 (also known as scavenger receptor B2) is a multifunctional receptor that  
24 mediates lipid uptake, advanced oxidation protein products, and immunological  
25 recognition, and has roles in lipid accumulation, apoptosis, as well as in metastatic  
26 colonization in cancer. CD36 is involved in tumor immunity, metastatic invasion, and  
27 therapy resistance through various molecular mechanisms. Targeting CD36 has  
28 emerged as an effective strategy for tumor immunotherapy. In this study, we have  
29 successfully generated a novel CD36 humanized mouse strain where the sequences  
30 encoding the extracellular domains of the mouse *Cd36* gene were replaced with the  
31 corresponding human sequences. The results showed that CD36 humanized mice only  
32 expressed human CD36, and the proportion of each lymphocyte was not significantly  
33 changed compared with wild-type mice. Furthermore, CD36 monoclonal antibody  
34 could significantly inhibit tumor growth after treatment. Therefore, the CD36  
35 humanized mice represent a validated preclinical mouse model for the evaluation of  
36 tumor immunotherapy targeting CD36.

37 **Keywords:** CD36; Colon cancer; Humanized mouse model; Immunotherapy;  
38 Monoclonal antibody

39

40

41

42

43

## 44 **Introduction**

45       The transmembrane protein CD36 is a membrane glycoprotein expressed on the  
46 cell surface in multiple cell types, including platelets, mononuclear phagocytes,  
47 adipocytes, hepatocytes, myocytes, and some epithelia[1]. Clinical studies have found  
48 significant upregulation of CD36 expression in tumor tissues of cervical cancer[2, 3],  
49 gastric cancer[4], hepatocellular carcinoma[5], and ovarian cancer[6], which promotes  
50 tumor growth, metastatic invasion, and therapy resistance of these tumors through  
51 CD36-mediated lipid metabolism.[7].

52       CD36 expression was significantly higher in primary Colorectal Cancer (CRC)  
53 tumor tissue than in normal colonic mucosa, and 5-year survival was lower in CRC  
54 patients with high CD36 mRNA expression than in those with low CD36 mRNA  
55 expression [8].CD36 is involved in CRC development by promoting proteasome-  
56 dependent ubiquitination of Glypcian 4 (GPC4) to inhibit the  $\beta$ -catenin/c-myc axis[9].  
57 The non-coding RNA (lncRNA) TINCR was found to inhibit miR-107 expression and  
58 activate CD36, which further inhibited CRC cell proliferation and promoted CRC cell  
59 apoptosis[10]. Inhibition of fatty acid synthase (FASN) was found to upregulate CD36  
60 expression in FASN knockout CRC cells and CRC models based on transgenic mice  
61 with hetero- and homozygous deletions of FASN, thereby promoting the proliferation  
62 of CRC cells[8]. CRC with high metastatic potential expresses higher levels of CD36,  
63 which promotes CRC metastasis by upregulating MMP28 and increasing E-  
64 calmodulin cleavage[11]. Lipid droplets (LD) are a common feature of cancer cell  
65 adaptation to tumour microenvironment (TME) acidosis and a key driver of increased

66 cancer cell aggressiveness[12]. It was found that acidosis of TME induces plasma  
67 membrane transport of CD36 via TGF- $\beta$ 2, which promotes LD formation and  
68 enhances metastasis and invasion of CRC[13]. Therefore, CD36 is closely associated  
69 with CRC development, growth, tumor immunity, and metastatic invasion, suggesting  
70 that inhibition of CD36 may be necessary to improve the efficacy of FASN-targeted  
71 therapy.

72 Humanized mice include immunodeficient mice xenografted with human cells or  
73 tissues as well as mice expressing human gene products[14]. Patient-derived  
74 xenografts or cell-derived xenografts (PDX/CDX) models based on immune  
75 reconstituted mice or target gene humanized mice are the most used for preclinical *in*  
76 *vivo* efficacy evaluation of antibodies for tumor immunotherapy. However, immune  
77 reconstituted mice have limitations such as species specificity of histocompatibility  
78 complex (MHC) antigens, underdevelopment of the immune system, impaired class  
79 switching and affinity maturation of immunoglobulins[15]. Therefore, a murine model  
80 used to conduct preclinical testing of anti-hCD36 Abs would be an invaluable tool for  
81 defining their mechanism of action and potential clinical utility. In this study, we  
82 described the generation and characterization of the humanized CD36(hCD36) mouse  
83 strain and validation of their use in studying CD36-targeting therapies for potential  
84 application in *in-vivo* anti-tumor activity.

## 85 **Materials and methods**

### 86 **Reagents and materials**

87 RP23-115H10 (cloned in the pBACe3.6 vector) and CH17-134L21 (cloned in the

88 pBACGK1.1 vector) were obtained from the BACPAC Resources Center at BACPAC  
89 Genomics. ShunRan biology provided MC38 (colon adenocarcinoma) cells, which  
90 were cultivated and maintained in Dulbecco's Modified Eagle's medium (DMEM)  
91 with 10% fetal bovine serum (FBS) at 37°C and 5% CO<sub>2</sub>. Antibodies against mouse  
92 cell-surface molecules including mCD45-BV510 (clone 30-F11), mGr-1- PerCP  
93 (clone RB6-8C5), mCD4-BV421 (clone GK1.5), mF4/80-FITC (clone BM8), mCD4-  
94 BV510 (clone RM4-5), mCD8a-PE (clone 53-6.7), mFoxp3-APC (clone FJK-16S),  
95 mCD19-FITC (clone 6D5), mTCR  $\beta$ chain- PerCP/Cy5.5 (clone H57-597), mCD11c-  
96 BV605 (clone N418), mCD11b-PE (clone M1/70), and mCD11b-V450 (clone V450)  
97 were purchased from Biolegend(USA). Antibodies against mouse cell-surface  
98 molecules including mCD3-V450 (clone 17A2), mNK1.1-PE-Cy7 (clone PK136),  
99 and mTCR  $\beta$ chain- APC (clone H57-597) were purchased from BD  
100 Pharmingen(USA). Antibody against mouse cell-surface molecule CD36 Monoclonal  
101 antibody-APC (clone HM36) was purchased from eBioscience. Antibody against  
102 human cell-surface molecule hCD36-PE (clone 5-271) was purchased from  
103 Biolegend(USA). Other reagents including anti-CD16/32, PE Mouse IgG2a, and  $\kappa$   
104 Isotype Ctrl(FC) Antibody (clone MOPC-173) were purchased from Biolegend(USA).  
105 Armenian Hamster IgG Isotype Control-APC (clone eBio299Arm) was purchased  
106 from Invitrogen.

## 107 **Animal experiments**

108 C57BL/6 mice were purchased from Biocytogen Pharmaceuticals (Jiangsu,  
109 China) Co., Ltd. Flp mice were purchased from Institute for Laboratory Animal

110 Resources, NIFDC. CD36 humanized mice (hCD36 mice) were provided by  
111 Biocytogen Pharmaceuticals (Beijing, China) Co., Ltd., production license No. SCXK  
112 (Su) 2021-0003. This study was carried out in strict accordance with the  
113 recommendations in the Guide for the Institutional Animal Care and Use Committees  
114 (IACUC) guidance. All animal studies were performed according to the protocol  
115 approved by the animal care and use committee of Biocytogen Pharmaceuticals  
116 (Approval number: PS-01-2203022). The SPF barrier facility kept the test animals at  
117 a constant temperature of ( $22 \pm 2^\circ\text{C}$ ), with a 12 h/12 h light/dark cycle, and were free  
118 access to food and drink. All surgery was performed under sodium pentobarbital  
119 anesthesia, and all efforts were made to minimize suffering. Mice were euthanized  
120 with  $\text{CO}_2$  to minimize or alleviate the animals' suffering.

## 121 **Construction of the hCD36 targeting vector**

122 On the C57BL/6J genetic background, a partial sequence of mouse exon 4 to a  
123 partial sequence of exon 15 of approximately 43 kb was replaced with a partial  
124 sequence of exon 3 to a partial sequence of exon 14 of approximately 27 kb  
125 containing the human *CD36* (Fig. 1A). Homology areas, human DNA, an Frt-flanked  
126 Neo resistance cassette, and a diphtheria toxin A (DTA) cassette were all included in  
127 the construction of the hCD36 targeting vector. The vectors pUNS-Neo-2G and pES-  
128 Fte were provided by Biocytogen Pharmaceuticals (Beijing, China) Co., Ltd. The  
129 mouse and human genomic DNA fragments of A, B, and C were amplified by PCR  
130 using DNA derived from Mouse BAC and Human BAC as templates. Primer designs  
131 for fragments A, B, and C are shown in Table S1. Intermediate vector 1 (pUNS-Neo-

132 2G-A1A2B1B2) and intermediate vector 2 (pES-FTe-C1-ORI-C2) were obtained by  
133 the Gibson assembly method, respectively. Intermediate vector 1 linearized by SmaI  
134 was electroporated into the mouse BAC which was modified by intermediate vector 2  
135 to obtain intermediate vector 3 (pES-FTe-LR-RR). Finally, the intermediate vector 3  
136 linearized by ScaI was electroporated to the human BAC(with Neo) to form the pES-  
137 Fe-ABC vector (the hCD36 targeting vector).

### 138 **Generation of humanized CD36 mice**

139 The correct targeting vector was transfected into C57BL/6J embryonic stem (ES)  
140 cells (Biocytogen Pharmaceuticals (Beijing) Co., Ltd.) by electroporation. G418-  
141 resistant ES clones were assayed using Southern Blot techniques to confirm the  
142 integration of the exogenous gene. The ES clone cells which had correct sequencing  
143 were injected into BALB/c blastocysts and implanted into pseudo pregnant females to  
144 produce F0 chimeric mice. F0 chimeric mice were mated with Flp mice to obtain F1  
145 heterozygous mice with the *Neo* allele deleted. Afterwards, F1 heterozygous mice  
146 were mated with each other to obtain hCD36 mice (Unless otherwise stated, hCD36  
147 mice below refer to homozygous hCD36 mice).

### 148 **Analysis of the hCD36 targeting vector, the ES cells, and the** 149 **F1 mice**

150 The hCD36 targeting vectors were subjected to restriction digestion analysis.  
151 These vectors were digested with ScaI (Thermo, FD0434), EcoRV (Thermo, FD0304),  
152 and NcoI (Thermo, FD0574), respectively. The vectors which conformed by the  
153 restriction digestion analysis would be sequenced for confirmation. The G418-

154 resistant ES clones were subjected to Southern Blot assay. We digested cellular DNA  
155 with ScaI(NEB, R3122S) or EcoNI(NEB, R0521S) and hybridized using 2 probes,  
156 respectively (Restriction enzyme digestion sites are shown in Fig. 1A; primer design  
157 of the probes is shown in Table S3). Identification of the DTA cassette in ES positive  
158 clones by PCR (The primer sequences were shown in Table S2). The ES clone cells  
159 which had correct sequencing were used for blastocyst injection. Somatic cells from  
160 female WT and F1 mice were collected for genotype identification by PCR (Primer  
161 design for genotype identification of F1 mice is shown in Table S4, and the  
162 identification strategy has been Fig. 1A). Genetic sequencing was performed on key  
163 positions of F1 mice screened by PCR. The correctly sequenced F1 mice were used  
164 for amplification and preparation of hCD36 mice.

### 165 **Analysis of human CD36 mRNA expression and full-length** 166 **Sanger sequencing of CDS (Coding DNA sequence) in** 167 **hCD36 mice**

168 Lung tissues of hCD36 mice and WT mice (C57BL/6 mice) were harvested for  
169 extracting total RNA using RNAprep Pure Cell / Bacteria Kit (TIANGEN, DP430).  
170 The mRNA expression of hCD36 and mCD36 was determined using GAPDH as the  
171 internal control. Primer annealing temperatures and the number of cycling were set as  
172 follows: initial 94 °C for 2 min, followed the first step by 15 cycles of 98 °C for 10 s,  
173 67 °C for 30 s, and 68 °C for 30 s, the second step by 25 cycles of 98 °C for 10 s,  
174 57 °C for 30 s, and 68 °C for 30 s; an additional extension at 68 °C for 5 min; and  
175 finally held at 16 °C. The primer sequences were shown in Table S5. The qualified

176 RNA was used for cDNA library construction. The cDNA obtained by reverse  
177 transcription was amplified by RT-PCR. Primer annealing temperatures and the  
178 number of cycling were set the same as for the amplification of *CD36* mRNA. Finally,  
179 qualified cDNA library was sequenced by the company GENEWIZ.

## 180 **Protein expression analysis of CD36 and** 181 **immunophenotyping in hCD36 mice**

182 CD36 expression was examined in bone marrow derived from WT mice and  
183 heterozygous hCD36 mice, and hCD36 mice (peritoneal exudative macrophages)  
184 using anti-mouse CD36 antibody-APC (Biolegend, 102611) and anti-mouse CD36-PE  
185 (eBioscience<sup>TM</sup>, 17-0362-82). And hCD36 was detected with an anti-human CD36  
186 antibody (Biolegend, 336205) in peritoneal exudative macrophages. We analyzed the  
187 expression of CD36 on immune cells in the blood of WT mice and hCD36 mice using  
188 flow cytometry. ACK lysis buffer (Beyotime, China) was first added to the  
189 anticoagulated blood to remove red blood cells. These cells were then co-incubated  
190 with a mixture of LD-NIR (Biolegend, USA) and anti-mCD16/32 (Biolegend, USA,  
191 clone 93) respectively for 10 min at 4°C for deadwood staining and blocking of non-  
192 specific binding. Finally, immune cells in these cell suspensions were stained at 4°C.  
193 After each staining, cells were washed with PBS to remove unbound labeled  
194 antibodies. After staining, multicolor flow cytometry of the cells was performed using  
195 Attune NxT (Thermo Fisher Scientific, USA), and analysis of the data was performed  
196 using FlowJo 10. We further analyzed the development, differentiation, and  
197 distribution of immune cells in the spleen, lymph nodes, and blood of WT mice and

198 hCD36 mice, respectively. The spleen cell suspensions and lymph node cell  
199 suspensions were processed and analyzed with the same procedure as anticoagulated  
200 blood.

## 201 **Routine mouse blood test**

202       Peripheral blood of female WT and hCD36 mice (n=8, 6-8 weeks old) was  
203 collected into EDTA blood collection tubes after anesthesia with sodium pentobarbital.  
204 The counts of red blood cells (RBC), white blood cells (WBC), neutrophils (NEUT#),  
205 lymphocytes (LYMPH#), monocytes (MONO#), hemoglobin (HGB), and platelets  
206 (PLT) in the peripheral blood of mice were determined using a fully automated  
207 modular blood fluid analyzer (Sysmes, XN-1000); the pressure of red blood cells  
208 (HCT), the mean red blood cell volume (MCV) and red blood cell distribution width  
209 (RDW); mean platelet volume (MPV), hemoglobin content (MCH) and mean  
210 hemoglobin concentration (MCHC).

## 211 **Biochemical examination of mouse peripheral blood**

212       Peripheral blood of female WT and hCD36 mice (n=8, 6-8 weeks old) was  
213 collected into heparin collection tubes after anesthesia with sodium pentobarbital, and  
214 the supernatant was collected after centrifugation. The concentrations of alanine  
215 aminotransferase (ALT), aspartate aminotransferase (AST), alkaline phosphatase  
216 (ALP), albumin (ALB), glucose (GLU), urea (UREA), creatinine (CREA), total  
217 cholesterol (TC), triglycerides (TG), total protein (TP), alkaline phosphatase (ALP),  
218 serum amylase (AMY), phosphorus (P), creatine kinase (CK), high-density  
219 lipoprotein (HDL-C) and low-density lipoprotein (LDL-C) in the peripheral blood of

220 mice were determined using a fully automatic biochemical analyzer (Hitachi, 3110).

## 221 ***In vivo* efficacy evaluation of CD36 monoclonal antibody**

222 Six- to eight-week-old humanized female hCD36 mice were housed in the  
223 specific-pathogen-free (SPF) barrier facility of the Animal Center of Biocytogen  
224 Pharmaceuticals (Beijing) Co., Ltd. in the individually ventilated cage. The  
225 experimental animals were acclimatized for 7 days before being used in experiments.  
226 5E5 Murine colon cancer MC38 cells were subcutaneously implanted into hCD36  
227 mice on the right dorsal side in a volume of 0.1ml per mouse. The tumor volume was  
228 measured once a day from day 0 after inoculation, and the tumor volume was  
229 calculated by the formula:  $0.5 \times \text{long diameter} \times \text{short diameter}^2$ . Mice were randomly  
230 grouped as tumors reached an average of 100 mm<sup>3</sup>. Then mice were treated with PBS,  
231 anti-CD36 chimeric human-mouse monoclonal antibody (subsequently abbreviated as  
232 1G04 which was made in house.) through i.p. injection. The antibody was  
233 administered three times a week for six consecutive doses. Animal well-being and  
234 behaviors were monitored once a day during the experiment process. We measured  
235 the tumor volume and weight of the animals twice weekly. The animals were  
236 euthanized at the end of the experiment, and the relative tumor growth inhibition (TGI)  
237 rate was measured. The antitumor efficacy is expressed as tumor growth inhibition in  
238 terms of tumor volume (TGI<sub>TV</sub>). The TGI<sub>TV</sub> in percent was calculated as below:  
239  $TGI_{TV}(\%) = [1 - (T_i - T_0)/(C_i - C_0)] \times 100$ ; Where  $T_i$  = mean tumor volume of the  
240 drug-treated group on the final day of the study,  $T_0$ = mean tumor volume of the drug-  
241 treated group on the first dosing day,  $C_i$  = mean tumor volume of the control group on

242 the final day of the study,  $C_0$ = mean tumor volume of the control group on the first  
243 dosing day.

## 244 **Statistical analyses**

245 Mean $\pm$ SEM was used to assess the results. Statistical analysis was performed  
246 using SPSS 19 and graphical plotting of data was performed using Graph Pad Prism 7  
247 software. Student's t-test and one-way analysis of variance (ANOVA) were used for  
248 the comparison of all data. Statistical significance was required to meet a  $P$  value <  
249 0.05. \*  $p < 0.05$ , \*\*  $p < 0.01$ , \*\*\*  $p < 0.001$ , and \*\*\*\*  $p < 0.0001$ .

## 250 **Results**

### 251 **Generation of humanized CD36 heterozygous mouse model**

252 The fragment size after ScaI digestion should be 30,955 bp, 8094 bp, 5618 bp,  
253 2801 bp, 856 bp, and 96 bp. The fragment size after EcoRV digestion should be  
254 40,001 bp, 4020 bp, 2203 bp, 1427 bp, 540 bp, and 229 bp. The fragment size after  
255 NcoI digestion should be 22015 bp, 10334 bp, 5337 bp, 3259 bp, 2678 bp, 1841 bp,  
256 910 bp, 758 bp, 571 bp, 378 bp, and 339 bp. As shown in Fig. 1B, the hCD36  
257 targeting vector No. 17 met the requirements of restriction digestion analysis and was  
258 then sequenced to confirm (data not shown). Southern Blot was performed on G418-  
259 resistant ES clones and the results showed that No. 1D02, No. 1D06, No. 2B04, No.  
260 2D02, No. 2D03, No. 3F05, No. 1D08, and No. 2E06 were positively confirmed (Fig.  
261 1C). Sequenced of these positive clones showed that the four positive clones No.  
262 2B04, No. 1D08, No. 2D03, and No. 3F05 were free of random insertions (data not  
263 shown). Finally, the correct ES-positive clones were injected into BALB/c blastocysts

264 and then implanted into pseudo pregnant females to produce F0 chimeric mice. F0  
265 chimeric mice were mated with Flp mice to obtain F1 heterozygous mice with the  
266 Neo allele deleted. Genotype identification of F1 mice somatic cells by PCR showed  
267 that the two mice No. F1-01 and No. F1-02 were both positive heterozygous mice  
268 (Fig. 1D). The maternal ES positive of mice No. F1-01 and F1-02 was No. 2D03, and  
269 PCR identified No. 2D03 without the DTA cassette (S1 Fig). In addition, one of the  
270 F1 mice which was sequenced at the critical position showed no random insertion (S4  
271 Fig). The F1 mice No. F1-01 and No. F1-02 were used for the amplification and  
272 preparation of hCD36 mice.

### 273 **Generation of hCD36 mouse model**

274 The hCD36 mice established based on the C57BL/6 mouse background were  
275 obtained by replacing exons 4 to part of 15 of the extracellular domains of CD36  
276 encoding the mouse with human exons 3 to 14 (Fig. 1A). The hCD36 mice were  
277 generated by mating F1 mice with each other. The full-length Sanger sequencing data  
278 of the CD36 CDS in hCD36 mice showed that the sequence of exon 4 to exon 15 of  
279 the mouse CD36 gene was correctly replaced with the sequence of exon 3 to exon 14  
280 of the human CD36 gene in hCD36 mice (S5 Fig). We assumed that homozygous  
281 hCD36 mice only express hCD36, while heterozygous hCD36 mice express both  
282 hCD36 and mCD36. We detected CD36 expression in the bone marrow of  
283 heterozygous hCD36 mice and found that it expressed both mCD36 and hCD36,  
284 while WT mice only expressed mCD36 (results not shown). We analyzed the  
285 expression of CD36 mRNA in the lung tissue of hCD36 mice by RT-PCR. The results

286 revealed that only hCD36 mRNA was detected in hCD36 mice compared to WT mice  
287 (Fig. 2A). We then examined hCD36 protein expression in peritoneal exudative  
288 macrophages of hCD36 mice and found that only mCD36 was detected in WT mice,  
289 while only hCD36 was detected in hCD36 mice (Fig. 2B).

290 We further evaluated the expression pattern of hCD36 on different immune  
291 populations in the humanized mice and compared it with the expression of hCD36  
292 protein in humans. Similar to the pattern found on human immune cells[16-20],  
293 hCD36 protein is expressed on macrophages, monocytes, granulocytes, DCs, NK  
294 Cells, B cells, CD8+ T cells, CD4+ T cells, and Tregs of hCD36 mice (Fig. 2C). The  
295 regulatory region of the CD36 gene was not replaced in hCD36 mice, and the  
296 expression of CD36 protein on peripheral blood immune cells of hCD36 mice should  
297 be consistent with that of WT mice. However, our results showed that hCD36 protein  
298 expression was elevated on macrophages, monocytes, granulocytes, DCs, NK cells, B  
299 cells, CD8+ T cells, CD4+ T cells, and Tregs in hCD36 mice compared to mCD36  
300 protein expression in WT mice (Fig. 2C). Actually, it has been shown that introns can  
301 enhance transcript levels in eukaryotes by elevating mRNA accumulation and  
302 affecting transcription speed, nuclear export, and transcript stability[21]. Transgenic  
303 mice carrying the human histone H4 promoter had more extensive tissue expression in  
304 response to stimulation with the mixed introns compared to controls[22]. Tissue-  
305 specific expression of the mouse CD21 gene is closely associated with the 5'1.6kb  
306 region within intron 1 of the CD21 gene[23]. In addition, introns that can be  
307 efficiently spliced may make very different contributions in the context of different

308 cells, different promoters, or different coding sequences[21]. It is therefore reasonable  
309 to suspect that the partial sequence of exon 3 to exon 14 of the human CD36 gene  
310 may contain introns that enhance the expression of hCD36 protein in hCD36 mice.  
311 Altogether, our data demonstrate that the hCD36 mice recapitulate the expression  
312 pattern of the human CD36 on peripheral blood mononuclear cells (PBMCs),  
313 supporting the use of this mouse to study human CD36 as the therapeutic target for  
314 immune therapy.

## 315 **Analysis of leukocyte subpopulations and T cell** 316 **subpopulations**

317 To further investigate whether the humanization of CD36 could affect the  
318 immune system of mice, we next analyzed the leukocyte subpopulation in the spleen  
319 of hCD36 mice by flow cytometry. As shown in Figs 3A and B, the development,  
320 differentiation, and distribution of leukocyte subpopulations such as T cells, B cells,  
321 natural killer cells (NK), monocytes, dendritic cells (DC), and mononuclear  
322 macrophages in the spleen of hCD36 mice were not statistically different from WT  
323 mice ( $p > 0.05$ ). T cell subpopulations such as CD4+ T cells, CD8+ T cells, and Treg  
324 cells in the spleen of hCD36 mice were also similar to WT mice ( $p > 0.05$ ) (Figs 3C  
325 and D). In addition, we further analyzed the development, differentiation, and  
326 distribution of leukocyte subpopulations and T cell subpopulations in the blood and  
327 lymph nodes of hCD36 mice. We found that leukocyte subpopulations and T cell  
328 subpopulations of blood and lymph nodes were not significantly changed as compared  
329 with WT mice ( $p > 0.05$ ). (S2 and S3 Figs). Collectively, these results indicate that the

330 development, differentiation, and distribution of immune cells in hCD36 mice are not  
331 impaired, and hCD36 mice possess normal immune functions.

### 332 **Analysis of routine blood and blood biochemistry**

333 CD36 expression in non-immune cells mainly includes platelets, immature  
334 erythrocytes, podocytes, skeletal muscle cells, adipocytes, and cardiomyocytes[24].  
335 We next examined whether blood cell composition and morphology were affected by  
336 CD36 humanization. As shown in Fig. 4A, hCD36 mice were measured similarly to  
337 WT mice, indicating that humanization does not alter hematocrit composition and  
338 morphology.

339 Notably, cardiomyocyte-specific CD36 knockout mice exhibited a significant  
340 reduction in cardiac FA uptake and intramyocardial TG content[25]. Hepatocyte-  
341 specific CD36 knockout mice exhibited high-fat diet-induced hepatic steatosis and  
342 diminished insulin resistance, and blood biochemical assays suggested a progressive  
343 decrease in AST and ALT[26]. CD36 also contributes to the progression of chronic  
344 kidney disease by mediating renal lipid deposition, lipid peroxidation, and  
345 endocytosis of multiple substances by renal cells[27]. Endothelial cell-specific CD36  
346 knockout mice also exhibit elevated triglyceride levels, reduced total cholesterol, and  
347 increased glucose clearance[28]. These studies suggest that CD36 is closely  
348 associated with the normal function and disease development of organs such as the  
349 heart, liver, and kidney in mice. We next evaluated the effect of CD36 humanization  
350 on the normal function of these organs in hCD36 mice. There was no difference in  
351 biochemistry parameters between hCD36 mice and WT mice, indicating that

352 humanization does not alter the health of organs such as the heart, liver, and kidney  
353 (Fig. 4B).

### 354 ***In vivo* efficacy evaluation of CD36 monoclonal antibody**

355 Currently, there are no antibodies that specially recognize hCD36 other than the  
356 1G04 (patent WO2021176424A1) which cross-recognizes the mCD36 and hCD36.  
357 1G04 is currently in the biological testing phase. This antibody is an anti-CD36  
358 human-mouse chimeric monoclonal antibody that was obtained by replacing the Fc  
359 region of the mouse antibody ONA-0-V1 with the Fc region of the human antibody  
360 IgG1[29]. The Fc region of 1G04 contains L234A/L235A (LALA) modification. The  
361 results of the proprietary ELISA assay showed that 1G04 exhibited similar affinity  
362 and binding properties for hCD36 and mCD36[29]. 1G04 can inhibit tumor growth by  
363 blocking the CD36-mediated lipid uptake of tumor cells[29]. To assess the cross-  
364 reactivity of 1G04, we examined its binding to mCD36/hCD36 *in vitro* by flow  
365 cytometry, and we confirmed that the 1G04 demonstrated comparable binding to both  
366 mCD36 and hCD36 (Fig. 5B). It was reported that 1G04 exhibited significant tumor  
367 inhibition in either C57BL/6 mice inoculated with MC38 cells or BALB/c nude mice  
368 inoculated with HCT-116 cells[29]. To demonstrate that the enhancement of anti-  
369 tumor immunity could be modulated by therapeutic blockade of CD36, hCD36 mice  
370 with established WT MC38 tumors were treated with 1G04 at 3mg/kg or 10mg/kg.  
371 Compared with the control group, 1G04 treatments at the dosage of 10mg/kg and  
372 3mg/ kg achieved significant TGI at 47.3% and 31.6%, respectively (Fig. 5C). And  
373 neither the low-dose group nor the high-dose group induced significant body weight

374 change in the experimental animals compared with the control group ( $p > 0.05$ )(Fig.  
375 5D). Therefore, we successfully validated the inhibitory effect of 1G04 on colon  
376 cancer tumor growth in hCD36 mice. The hCD36 mice could be used for preclinical  
377 *in vivo* efficacy evaluation of anti-hCD36 antibody.

## 378 **Discussion**

379 CD36 is actively involved in the growth, tumor immunity, metastatic invasion,  
380 and drug resistance of various tumors through lipid metabolism[30]. Blocking CD36-  
381 mediated lipid metabolism is a strategy that can be considered for future tumor  
382 therapy. However, a lack of mouse models that faithfully recapitulate the human  
383 expression patterns of hCD36 has hindered progress in evaluating the anti-tumor  
384 effect of hCD36-targeting antibodies *in vivo*. Here, we developed a hCD36 mouse  
385 model by replacing the extracellular region of mCD36 with the human counterpart,  
386 which allowed for testing the therapeutic potential of anti-hCD36-targeting antibody.  
387 Expression of hCD36 was only detectable in hCD36 mice while mCD36 was not  
388 expressed. Next, the distribution of lymphocyte subpopulations in the blood, lymph  
389 nodes, and spleen of the hCD36 mice was consistent with that of WT mice, indicating  
390 that humanized mice did not affect the distribution of lymphocyte subpopulations.  
391 Furthermore, the immune function, blood cell composition and morphology, and vital  
392 organ function were not affected by humanization.

393 We further validated the inhibitory effect of 1G04 on colon cancer tumors in  
394 hCD36 mice. Our data showed that targeting the hCD36 with blocking antibody was a  
395 promising strategy to enhance antitumor immunity and reduce tumor burden.

396 However, most of the development of CD36 antibodies is in the preclinical and  
397 biological testing stage, and there are few CD36 antibodies whose clinical indications  
398 are used for tumor immunotherapy. Although it is a limitation of validation of the  
399 hCD36 mice due to lacking of specially recognizing human CD36 monoclonal  
400 antibodies, this implies that there is much deeper research on CD36 to develop  
401 human-specific CD36 antibodies. In addition, with the emergence of drugs utilized for  
402 metabolic inflammatory syndrome and the cardiovascular class of targeting CD36  
403 antibodies in the future, hCD36 mice could also be able to further accelerate the  
404 development of this field of antibodies from preclinical to clinical progress. In fact,  
405 the use of humanized mice in human metabolic inflammatory syndrome and  
406 cardiovascular disease research includes the exploration of mechanisms of action,  
407 preclinical pharmacodynamic and toxicological evaluation, and target discovery[14,  
408 31-33]. Therefore, hCD36 mice could also further discover the potential association  
409 of CD36 with different targets in several diseases, thus facilitating drug development  
410 for these diseases.

## 411 **Conclusion**

412 We have successfully generated hCD36 mice by a genetic engineering approach  
413 and validated the inhibitory effect of 1G04 on colon cancer tumor growth in these  
414 mice. The hCD36 mice should be a valuable preclinical mouse model for the  
415 evaluation of tumor immunotherapy targeting CD36.

## 416 **Authorship contributions**

417 Xiulong Xie: Validation, Formal analysis, Writing - Original Draft. Zhenlan Niu:

418 Resources, Analysis and interpretation of data, Writing- Reviewing and Editing.  
419 Linlin Wang: Conception and design of the study, Acquisition of data, Analysis and  
420 interpretation of data. Xiaofei Zhou: Project administration. Xingyan Yu:  
421 Investigation. Hongyan Jing: Visualization. Yi Yang: Funding acquisition, Writing-  
422 Reviewing and Editing.

## 423 Sources of Founding

424 This work was supported by Shandong Province Antibody Drug Innovation and  
425 Entrepreneurship Community [grant numbers 2021CXCYGTT16].

## 426 References

- 427 1. Silverstein RL, Febbraio M. CD36, a scavenger receptor involved in immunity, metabolism, angiogenesis, and  
428 behavior. *Sci Signal*. 2009;2(72):re3. doi: 10.1126/scisignal.272re3.
- 429 2. Deng M, Cai X, Long L, Xie L, Ma H, Zhou Y, et al. CD36 promotes the epithelial-mesenchymal transition and  
430 metastasis in cervical cancer by interacting with TGF- $\beta$ . *J Transl Med*. 2019;17(1):352. doi: 10.1186/s12967-019-  
431 2098-6.
- 432 3. Yang P, Su C, Luo X, Zeng H, Zhao L, Wei L, et al. Dietary oleic acid-induced CD36 promotes cervical cancer  
433 cell growth and metastasis via up-regulation Src/ERK pathway. *Cancer Lett*. 2018;438:76-85. doi:  
434 10.1016/j.canlet.2018.09.006.
- 435 4. Pan J, Fan Z, Wang Z, Dai Q, Xiang Z, Yuan F, et al. CD36 mediates palmitate acid-induced metastasis of  
436 gastric cancer via AKT/GSK-3 $\beta$ / $\beta$ -catenin pathway. *J Exp Clin Cancer Res*. 2019;38(1):52. doi: 10.1186/s13046-  
437 019-1049-7.
- 438 5. Luo X, Zheng E, Wei L, Zeng H, Qin H, Zhang X, et al. The fatty acid receptor CD36 promotes HCC  
439 progression through activating Src/PI3K/AKT axis-dependent aerobic glycolysis. *Cell Death Dis*. 2021;12(4):328.  
440 doi: 10.1038/s41419-021-03596-w.
- 441 6. Ladanyi A, Mukherjee A, Kenny HA, Johnson A, Mitra AK, Sundaresan S, et al. Adipocyte-induced CD36  
442 expression drives ovarian cancer progression and metastasis. *Oncogene*. 2018;37(17):2285-301. doi:  
443 10.1038/s41388-017-0093-z.
- 444 7. Wang J, Li Y. CD36 tango in cancer: signaling pathways and functions. *Theranostics*. 2019;9(17):4893-908. doi:  
445 10.7150/thno.36037.
- 446 8. Drury J, Rychahou PG, He D, Jafari N, Wang C, Lee EY, et al. Inhibition of Fatty Acid Synthase Upregulates  
447 Expression of CD36 to Sustain Proliferation of Colorectal Cancer Cells. *Front Oncol*. 2020;10:1185. doi:  
448 10.3389/fonc.2020.01185.
- 449 9. Fang Y, Shen ZY, Zhan YZ, Feng XC, Chen KL, Li YS, et al. CD36 inhibits beta-catenin/c-myc-mediated  
450 glycolysis through ubiquitination of GPC4 to repress colorectal tumorigenesis. *Nat Commun*. 2019;10(1):3981. doi:  
451 10.1038/s41467-019-11662-3.
- 452 10. Zhang X, Yao J, Shi H, Gao B, Zhang L. LncRNA TINCR/microRNA-107/CD36 regulates cell proliferation

453 and apoptosis in colorectal cancer via PPAR signaling pathway based on bioinformatics analysis. *Biol Chem.*  
454 2019;400(5):663-75. doi: 10.1515/hsz-2018-0236.

455 11. Drury J, Rychahou PG, Kelson CO, Geisen ME, Wu Y, He D, et al. Upregulation of CD36, a Fatty Acid  
456 Translocase, Promotes Colorectal Cancer Metastasis by Increasing MMP28 and Decreasing E-Cadherin  
457 Expression. *Cancers (Basel)*. 2022;14(1). doi: 10.3390/cancers14010252.

458 12. Schwartzburd P. Lipid droplets: could they be involved in cancer growth and cancer–microenvironment  
459 communications? *Cancer Commun (Lond)*. 2021;42(2):83-7. doi: 10.1002/cac2.12257.

460 13. Corbet C, Bastien E, Santiago de Jesus JP, Dierge E, Martherus R, Vander Linden C, et al. TGFbeta2-induced  
461 formation of lipid droplets supports acidosis-driven EMT and the metastatic spreading of cancer cells. *Nat*  
462 *Commun*. 2020;11(1):454. doi: 10.1038/s41467-019-14262-3.

463 14. Stripecte R, Munz C, Schuringa JJ, Bissig KD, Soper B, Meeham T, et al. Innovations, challenges, and  
464 minimal information for standardization of humanized mice. *EMBO Mol Med*. 2020;12(7):e8662. doi:  
465 10.15252/emmm.201708662.

466 15. Allen TM, Brehm MA, Bridges S, Ferguson S, Kumar P, Mirochnitchenko O, et al. Humanized immune system  
467 mouse models: progress, challenges and opportunities. *Nat Immunol*. 2019;20(7):770-4. doi: 10.1038/s41590-019-  
468 0416-z.

469 16. Y C, J Z, WG C, RL S. CD36, a signaling receptor and fatty acid transporter that regulates immune cell  
470 metabolism and fate. *J Exp Med*. 2022;219(6):e20211314. doi: 10.1084/jem.20211314.

471 17. C L-G, MP C, AL G, JL F, D B, J F. A simple method for detection of major phenotypic abnormalities in  
472 myelodysplastic syndromes expression of CD56 in CMML. *Haematologica*. 2007;92(6).

473 18. He C, Wang S, Zhou C, He M, Wang J, Ladds M, et al. CD36 and LC3B initiated autophagy in B cells  
474 regulates the humoral immune response. *Autophagy*. 2021;17(11):3577-91. doi: 10.1080/15548627.2021.1885183.

475 19. Albert ML, Pearce SF, Francisco LM, Sauter B, Roy P, Silverstein RL, et al. Immature dendritic cells  
476 phagocytose apoptotic cells via alphavbeta5 and CD36, and cross-present antigens to cytotoxic T lymphocytes. *J*  
477 *Exp Med*. 1998;188(7):1359-68. doi: 10.1084/jem.188.7.1359.

478 20. Chen Q, Ye W, Jian Tan W, Mei Yong KS, Liu M, Qi Tan S, et al. Delineation of Natural Killer Cell  
479 Differentiation from Myeloid Progenitors in Human. *Sci Rep*. 2015;5:15118. doi: 10.1038/srep15118.

480 21. Shaul O. How introns enhance gene expression. *The international journal of biochemistry & cell biology*.  
481 2017;91(Pt B):145-55. doi: 10.1016/j.biocel.2017.06.016.

482 22. Choi T, Huang M, Gorman C, Jaenisch R. A generic intron increases gene expression in transgenic mice.  
483 *Molecular and cellular biology*. 1991;11(6):3070-4. doi: 10.1128/mcb.11.6.3070-3074.1991.

484 23. Hu H, Martin BK, Weis JJ, Weis JH. Expression of the murine CD21 gene is regulated by promoter and  
485 intronic sequences. *J Immunol*. 1997;158(10):4758-68.

486 24. Zhang X, Fan J, Li H, Chen C, Wang Y. CD36 Signaling in Diabetic Cardiomyopathy. *Aging Dis*.  
487 2021;12(3):826-40. doi: 10.14336/ad.2020.1217.

488 25. Nagendran J, Pulinilkunnil T, Kienesberger PC, Sung MM, Fung D, Febbraio M, et al. Cardiomyocyte-specific  
489 ablation of CD36 improves post-ischemic functional recovery. *J Mol Cell Cardiol*. 2013;63:180-8. doi:  
490 10.1016/j.yjmcc.2013.07.020.

491 26. Zeng H, Qin H, Liao M, Zheng E, Luo X, Xiao A, et al. CD36 promotes de novo lipogenesis in hepatocytes  
492 through INSIG2-dependent SREBP1 processing. *Mol Metab*. 2022;57:101428. doi:  
493 10.1016/j.molmet.2021.101428.

494 27. Yang X, Okamura DM, Lu X, Chen Y, Moorhead J, Varghese Z, et al. CD36 in chronic kidney disease: novel  
495 insights and therapeutic opportunities. *Nat Rev Nephrol*. 2017;13(12):769-81. doi: 10.1038/nrneph.2017.126.

496 28. Daquinag AC, Gao Z, Fussell C, Immaraj L, Pasqualini R, Arap W, et al. Fatty acid mobilization from adipose

497 tissue is mediated by CD36 posttranslational modifications and intracellular trafficking. JCI Insight. 2021;6(17).  
498 doi: 10.1172/jci.insight.147057.

499 29. AZNAR BS, DE FM, SALVADOR G, VALERIE V, BEA M. ANTI-CD36 ANTIBODIES AND THEIR USE  
500 TO TREAT CANCER.  
501 [https://worldwidespacenetcom/publicationDetails/biblio?II=0&ND=3&adjacent=true&locale=en\\_EP&FT=D&date=20210910&CC=WO&NR=2021176424A1&KC=A1](https://worldwidespacenetcom/publicationDetails/biblio?II=0&ND=3&adjacent=true&locale=en_EP&FT=D&date=20210910&CC=WO&NR=2021176424A1&KC=A1). US2021.  
502

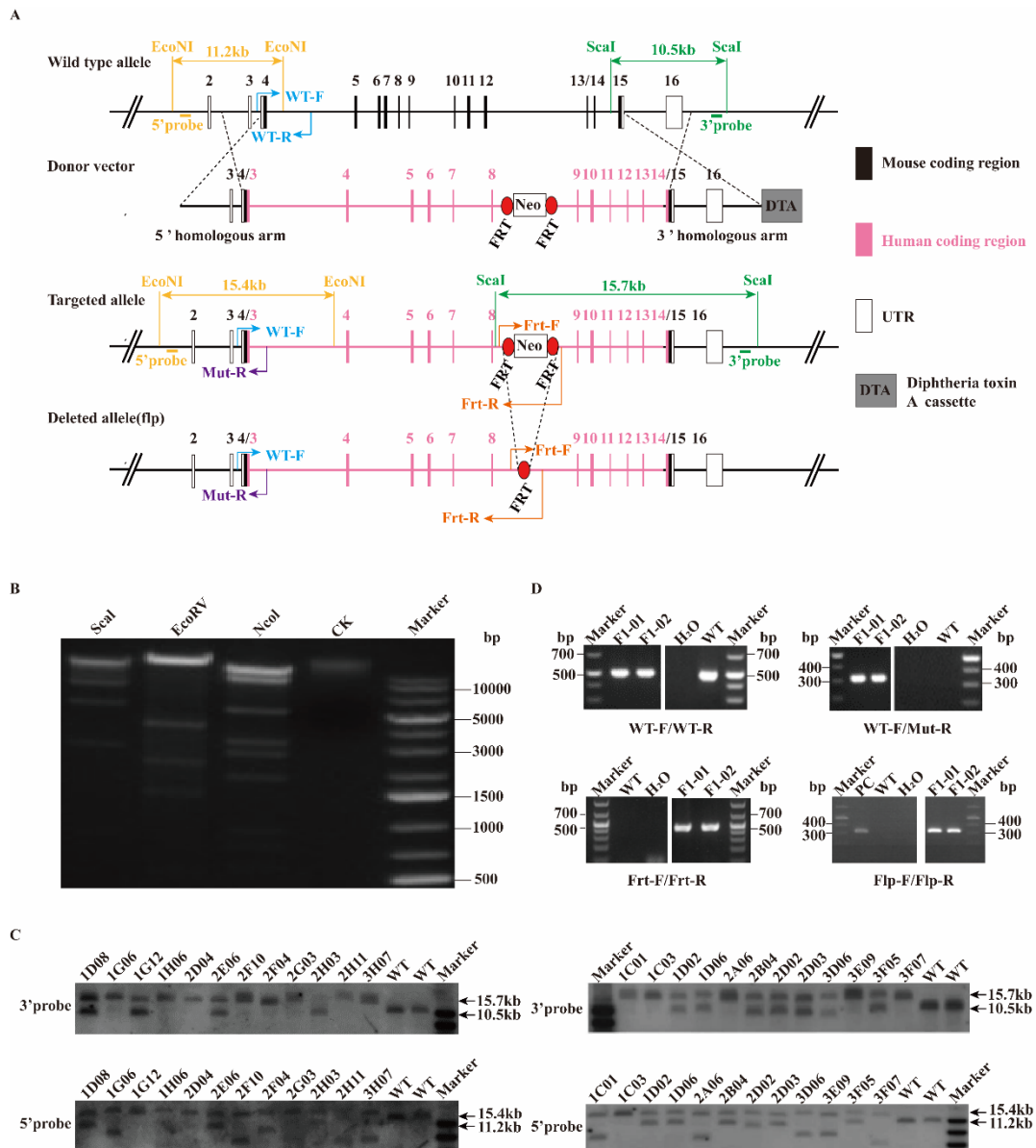
503 30. Ruan C, Meng Y, Song H. CD36: an emerging therapeutic target for cancer and its molecular mechanisms. J  
504 Cancer Res Clin Oncol. 2022;148(7):1551-8. doi: 10.1007/s00432-022-03957-8.

505 31. Ye W, Chen Q. Potential Applications and Perspectives of Humanized Mouse Models. Annual review of animal  
506 biosciences. 2022;10:395-417. doi: 10.1146/annurev-animal-020420-033029.

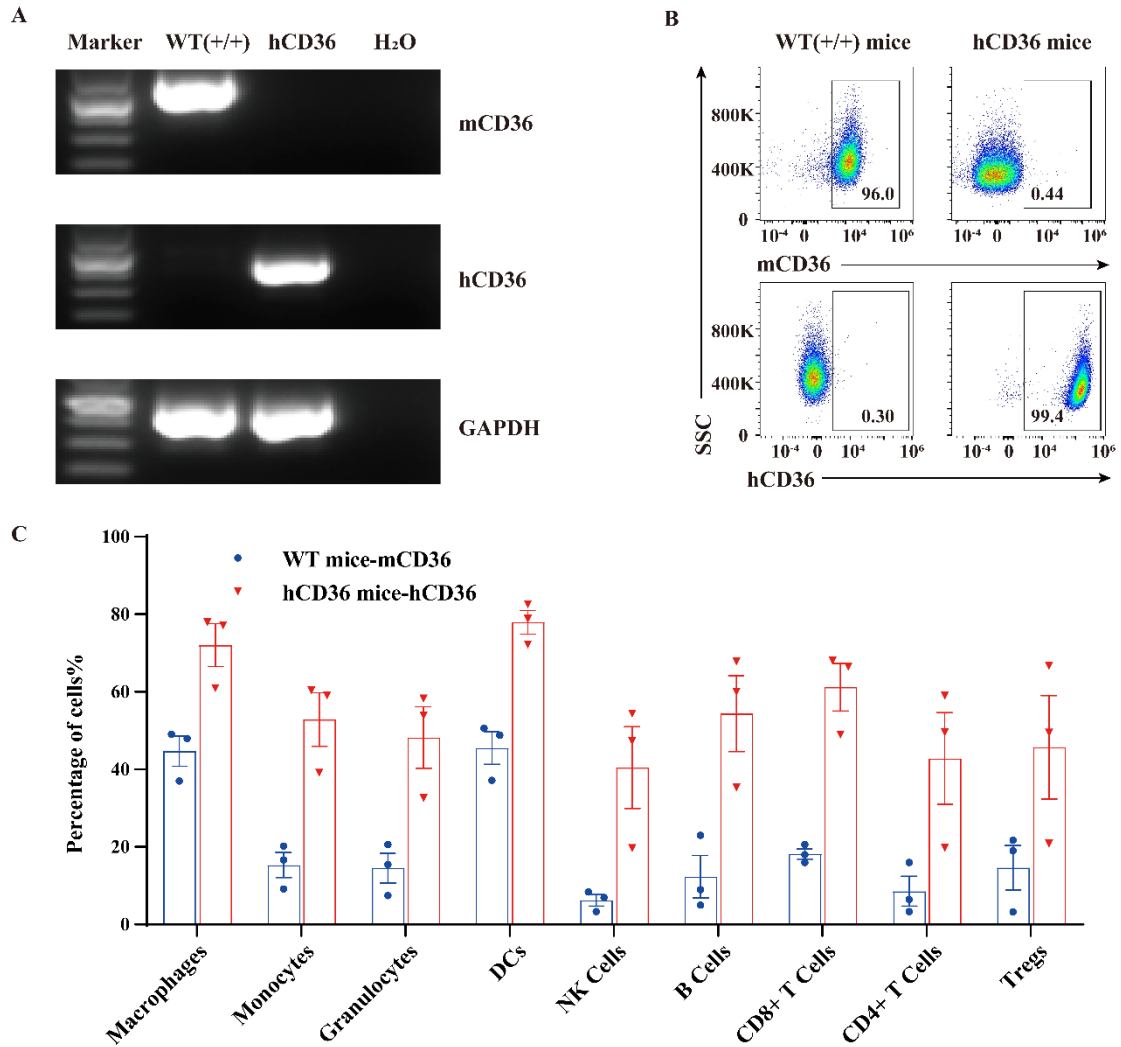
507 32. Scheer N, Wilson ID. A comparison between genetically humanized and chimeric liver humanized mouse  
508 models for studies in drug metabolism and toxicity. Drug Discov Today. 2016;21(2):250-63. doi:  
509 10.1016/j.drudis.2015.09.002.

510 33. Walsh NC, Kenney LL, Jangalwe S, Aryee KE, Greiner DL, Brehm MA, et al. Humanized Mouse Models of  
511 Clinical Disease. Annu Rev Pathol. 2017;12:187-215. doi: 10.1146/annurev-pathol-052016-100332.

512



513 **Fig 1. Characterization of the humanized CD36 heterozygous mouse model.** A:  
 514 Generation of the hCD36 mouse strain; B: Restriction digestion analysis of the  
 515 hCD36 targeting vector No. 17; C: Southern Blot analysis of ES positive clones; D:  
 516 PCR identification of the genotypes of F1 mice.



517

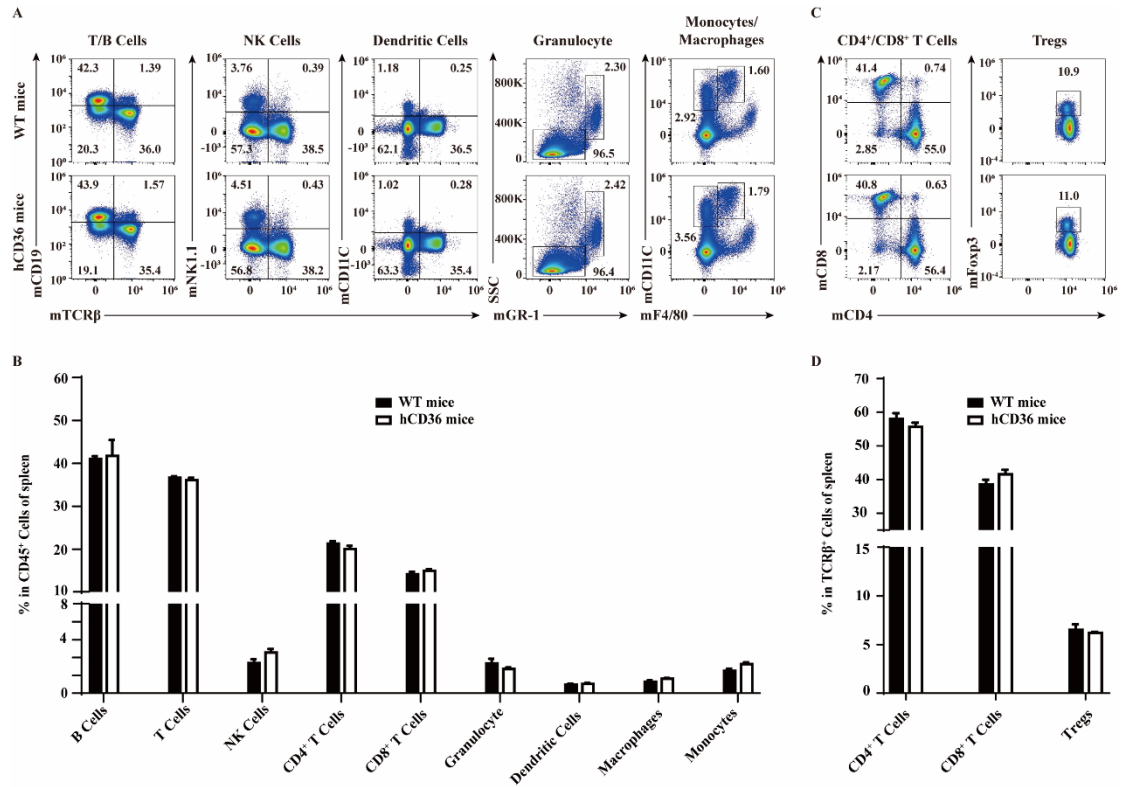
518 **Fig 2. Characterization of the hCD36 mouse model.** A: Expression of CD36

519 mRNA in hCD36 mice; B: Expression of CD36 on peritoneal exudative macrophages

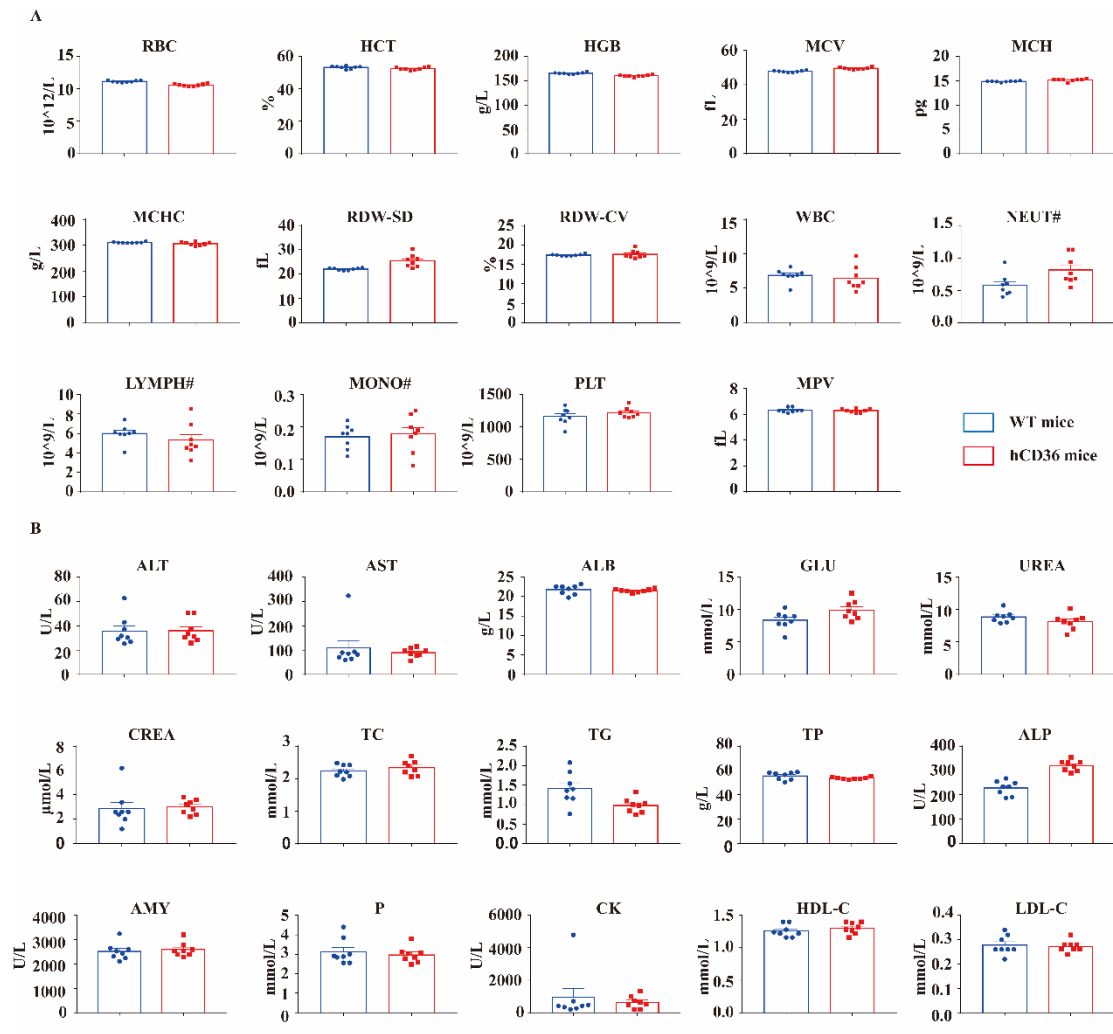
520 in hCD36 mice (n=1,7-week-old) ; C: Expression of CD36 on immune cells in the

521 blood of WT mice and hCD36 mice(n=3,8-week-old).

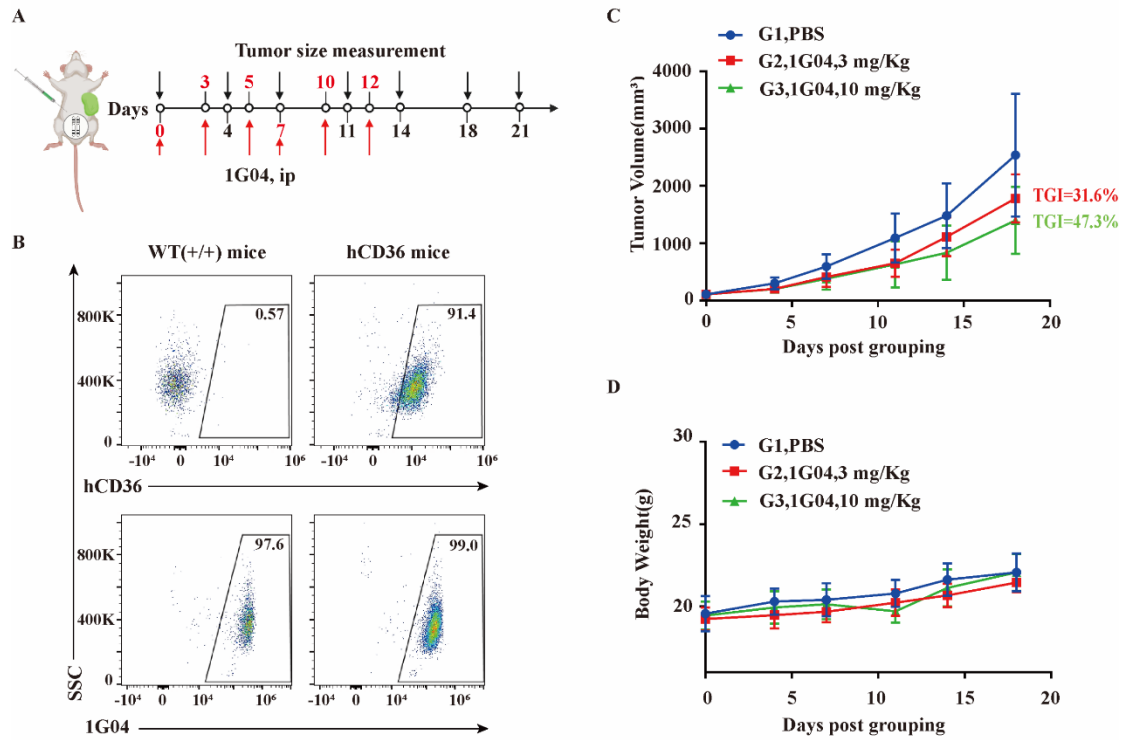
522



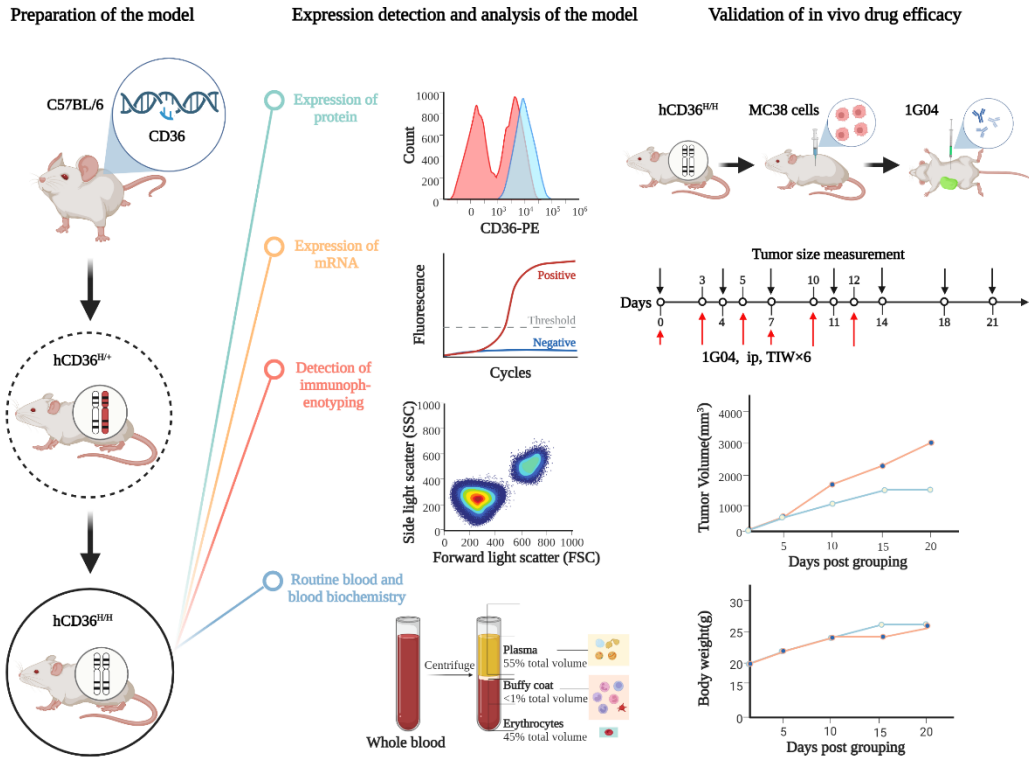
523 **Fig 3. Analysis of immune cells subpopulation in the spleen of hCD36 and WT**  
 524 **mice(n=3,8-week-old).** A, B: The frequency of T cells, B cells, NK cells, Monocyte,  
 525 DC cell, and macrophage cells in mCD45 cells. C, D: The frequency of CD4+ T cells,  
 526 CD8+ T cells, and Treg cells in mCD3 cells.



527 **Fig 4. Analysis of complete blood count and blood biochemical in hCD36 and WT**  
 528 **mice (n=8,6~8-week-old).** A: Analysis of complete blood count in mice; B: Analysis  
 529 of blood biochemistry in mice.



530 **Fig 5. Validation of the efficacy of 1G04 in hCD36 mice (n=6,6-8-week-old).** A:  
 531 Design of *in vivo* drug efficacy programs; B: Analysis of the *in vitro* binding of 1G04  
 532 to CD36. C: Tumor volume measurement during the treatment. D: Body weight  
 533 record during the treatment.



534 Fig 6. Graphical abstract.

535

536

537

538

539

540

541

542

543

544

545

546

547 **Supplementary data**

548 The following are the Supplementary data to this article:

549 **Table S1. Primer designs for fragments A, B, and C**

Primer	Sequence (5'-3')	Product size(bp)	Template
A1-F	CCTAAGAATACTCTACGGTCACATACCCCCCGGG TGGAGAACTAGATAGGGCGTG	593	Mouse
A1-R	GATAAGCAGGTCTCCGACTGGCATGAGAATGCCT CCAAAC		BAC
A2-F	ATTCTCATGCCAGTCGGAGACCTGCTTATCCAGA AGAC	342	Human
A2-R	TCCGATTCGCCAGATGATAAGGAACAGTACTAAC ATGCATACCTGTAGACAGC		BAC
B1-F	AACTCCGAGCCCTTCCACCAGTACTCTATCTGGC ACTTAATTGCC	277	Human
B1-R	CCATGCCAAGGAGGTTTATTTTTCCAGTACTTG AC		BAC
B2-1-F	CTGGAAAAATAAACCTCCTTGGCATGGTAGAGAT GGCCT	735	Mouse
B2-1-R	CTAATATATAAAAAGGCGTGTACAATTTTGCCAA AACTC		BAC
B2-2-F	TTGTACACGCCTTTTTATATATTAGTGACCACTGT G	590	Mouse
B2-2-R	GAAATGTCAGAGCCAGCGTCTTGCCCGGGTGAC ACAAATGATCCAGAAC		BAC
C1-F	AATTTACACAGGAGGCGCGCCTCGAGCAACTG AATCCTTACCATCTTCTGCC	322	Mouse
C1-R	GAGGGCTTACCGCTTACTAGTCACGTGTCTACAT CCCAGCCACATCACA		BAC
C2-F	GGTTTCCTTGTCGTAGATCTCACGTGTTCTATCTG AGATTCTGTGTCC	542	Mouse
C2-R	GTAAACTCCTCTTCAGACCTGGCGGCCGCCAC ATGCAGTGCAGAAGGGTGCA		BAC

550

551

552 **Table S2. Primer design for identification of DTA cassette in ES positive clones**

Primer	Sequence (5'-3')	Product size(bp)
DTA-F1	CTGGTACACAAGGAAATTATGACGATG	515
DTA-R1	GGTAGTTTGTCCAATTATGTCACACC	
DTA-F2	GAGGCGTGGTCAAAGTGACGTATCC	344
DTA-R2	CCTGACACGATTCCTGCACAGGC	

553

554 **Table S3. Primer design for Southern Blot confirmation of homologous**  
 555 **recombination in ES cells**

Probe	Sequence (5'-3')
5'Probe-F	5'-AGATAACAGGCTGGCCTGGAGAAAA -3'
5'Probe-R	5'-GTTGCCCAATACCATAATTTGGAAAAGT-3'
3'Probe-F	5'-CTTTAGCACCAGGTGTGCGTCAGTA-3'
3'Probe-R	5'-GGTCATGCACCAACATCCACACAAC-3'

556

557 **Table S4. Primer design for genotype identification of F1 mice**

Primer	Sequence (5'-3')	Product size(bp)
WT-F	AACCAGTGCTCTCCCTTGATTCTG	WT: 504
WT-R	AAAGCATGCCAGTCTACTCCAGA	
WT-F	AACCAGTGCTCTCCCTTGATTCTG	Mut: 315
Mut-R	GTCGCATCATATAGAGTTGCAGTGG	
Frt-F	TTGCCATGGATCATAGCTGTAGC	Mut-Flp: 490
Frt-R	AGTTACATATGGCTGGCGGCTGCT	(Deleted Neo)
Flp-F2	GACAAGCGTTAGTAGGCACATATAC	Mut: 325
Flp-R2	GCTCCAATTTCCCACAACATTAGT	

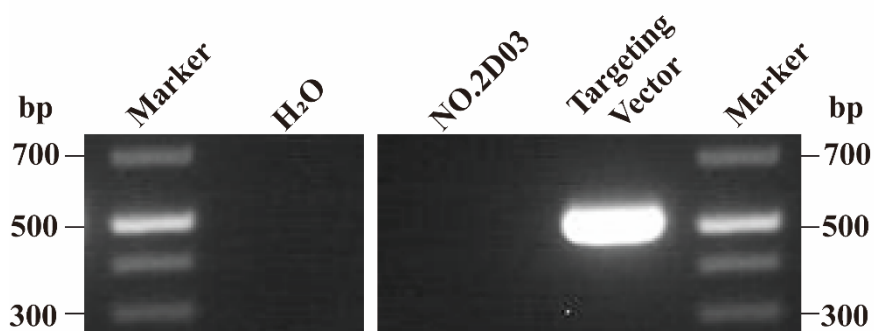
558

559

560 **Table S5. Primer design for CD36 mRNA expression analysis in hCD36 mice**

Primer	Sequence (5'-3')	Product size(bp)
mCD36-F	AAACCCAGATGACGTGGCAA	WT: 634
mCD36-R	TTCAGATCCGAACACAGCGT	
hCD36-F	AATGTAACCCAGGACGCTGA	Mut: 463
hCD36-R	GTGGAAATGAGGCTGCATCTG	
GAPDH-F	TCACCATCTTCCAGGAGCGAGA	WT: 479
GAPDH-R	GAAGGCCATGCCAGTGAGCTT	

561



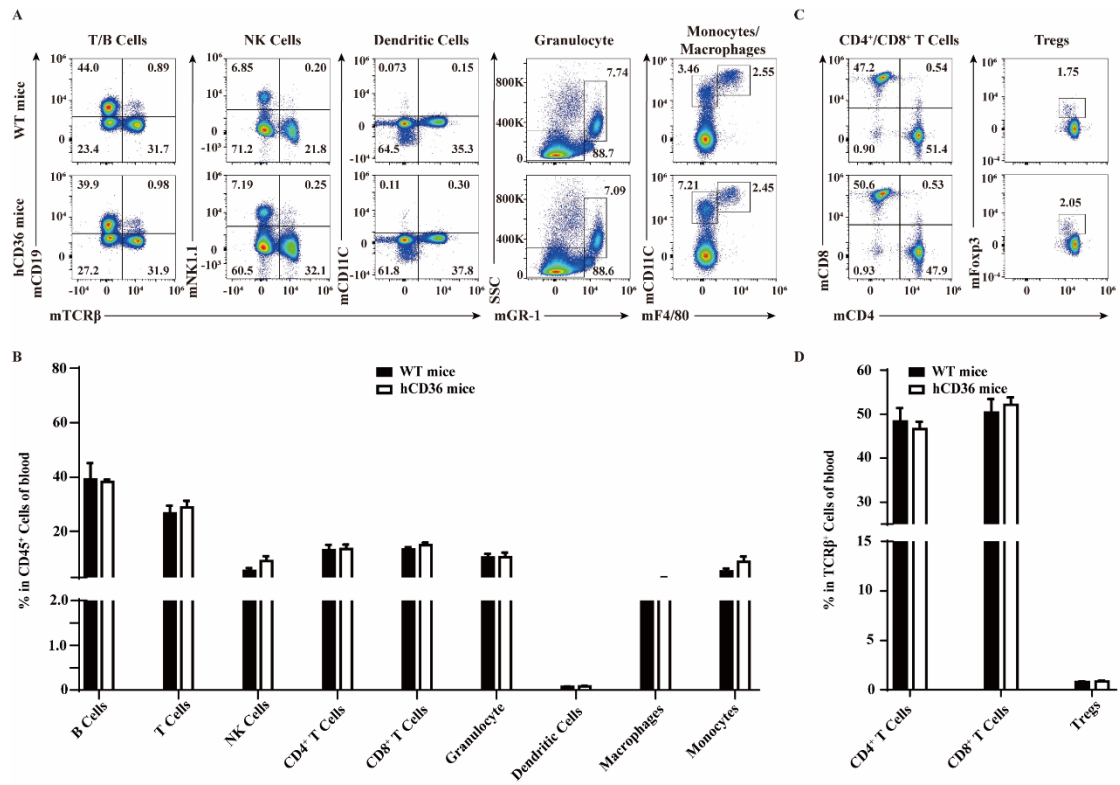
562

563 **S1 Fig. PCR identification of DTA cassette in targeting vectors and ES-positive**  
 564 **clones No. 2D03.**

565

566

567

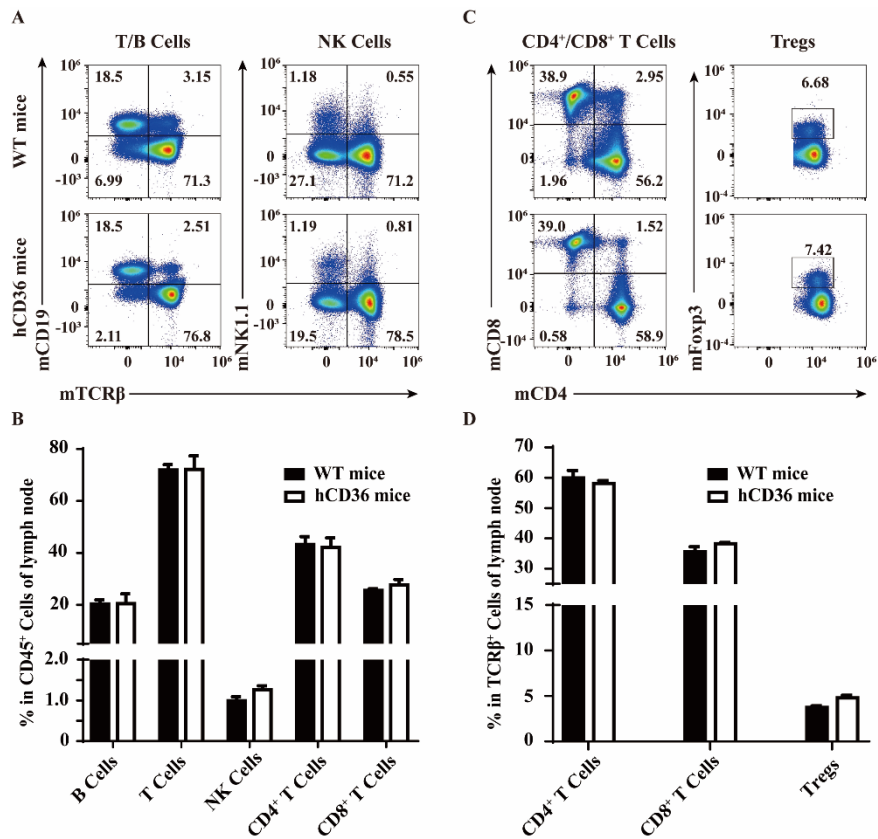


568 **S2 Fig. Analysis of immune cells subpopulation in the blood of hCD36 and WT**  
 569 **mice(n=3,8-week-old).** A, B: The frequency of T cells, B cells, NK cells, Monocyte,  
 570 DC cell, and macrophage cells in mCD45 cells. C, D: The frequency of CD4+ T cells,  
 571 CD8+ T cells, and Treg cells in mCD3 cells.

572

573

574



575 **S3 Fig. Analysis of immune cells subpopulation in the lymph nodes of hCD36**

576 **and WT mice(n=3,8-week-old). A, B: The frequency of T cells, B cells, NK cells in**

577 **mCD45 cells. C, D: The frequency of CD4<sup>+</sup> T cells, CD8<sup>+</sup> T cells, and Treg cells in**

578 **mCD3 cells.**

579

580

581

582

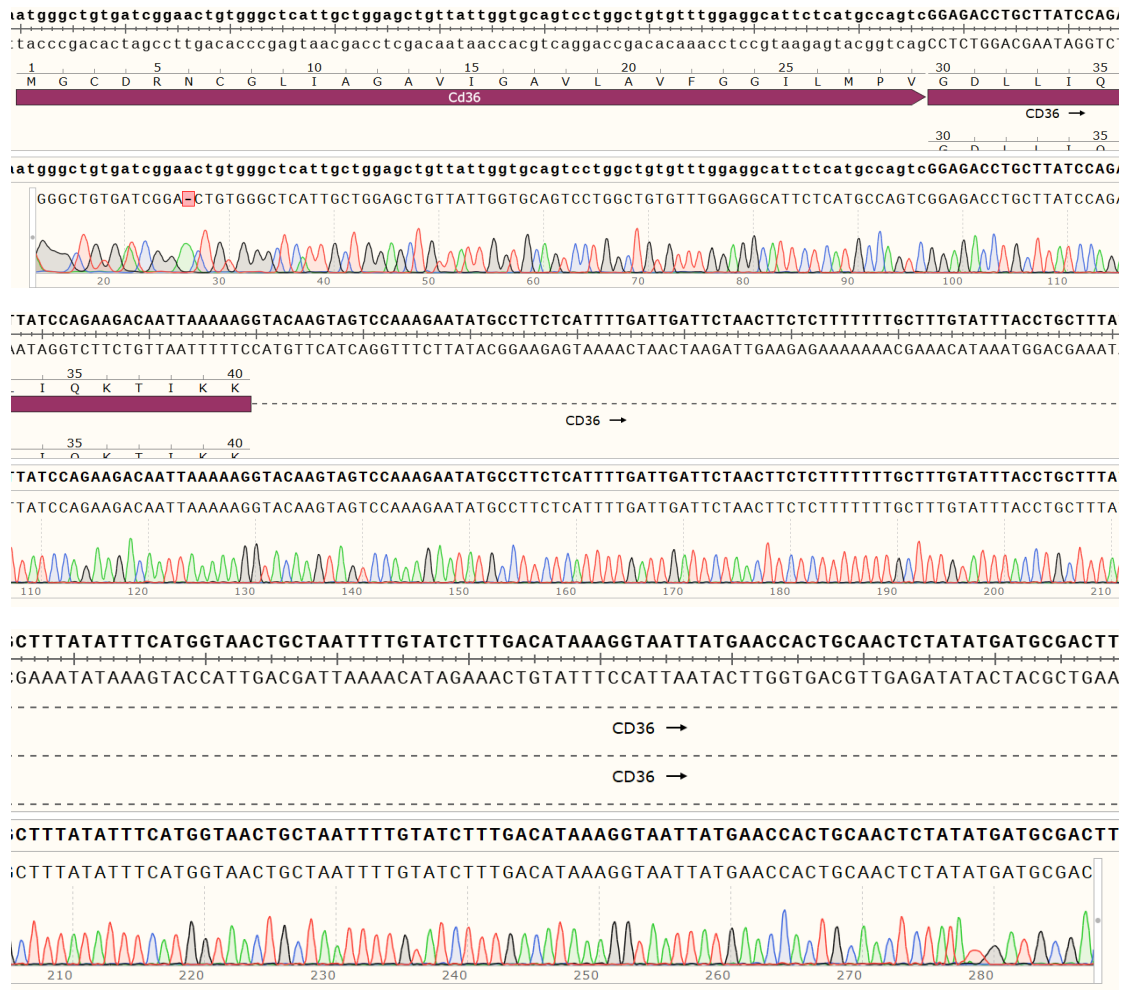
583

584

585

586

587



591 **S4 Fig. One of the F1 mice which was sequenced at the critical position showed**  
 592 **no random insertion.**

593  
 594  
 595  
 596  
 597  
 598  
 599

aatgggctgtgatcggaactgtgggctcattgctggagctgttattgggtcagctcctggctgtgtttggaggcatttctcatgccagtcggagacctgcttaccagaa  
 taccgcacactagccttgacaccgagtaacgacctgcacaataaccagctcaggaccgacacaaaacctccgtaagagtagcgtcagcctctggagcaataggctctt  
 1 5 10 15 20 25 30 35  
 Met Gly Cys Asp Arg Asn Cys Gly Leu Ile Ala Gly Ala Val Ile Gly Ala Val Leu Ala Val Phe Gly Gly Ile Leu Met Pro Val Gly Asp Leu Leu Ile Gln Ly

600

aatgggctgtgatcggaactgtgggctcattgctggagctgttattgggtcagctcctggctgtgtttggaggcatttctcatgccagtcggagacctgcttaccagaa  
 AATGGGCTGTGATCGGAACCTGTGGGCTCATTGCTGGAGCTGTTATTGGTGCAGTCTCGGCTGTGTTTGGAGGCATTCTCATGCCAGTCGGAGACCTGCTTACCAGAA  
 cagaagacaatataaaagcaagttgtcctcgaagaaggtaacaattgcttttaaaaattgggttaaacaggccacagaagtttacagacagtttggatctttgatgtg  
 gtctctgttaattttctgttcaacaggagctcttccatgtaacgaaatttttaaccaattttgtccgtgtctcaaatgtctgtcaaacctagaactacac  
 35 40 45 50 55 60 65 70  
 Gln Lys Thr Ile Lys Lys Gln Val Val Leu Glu Glu Gly Thr Ile Ala Phe Lys Asn Trp Val Lys Thr Gly Thr Glu Val Tyr Arg Gln Phe Thr Ile Phe Asp Val

cagaagacaatataaaagcaagttgtcctcgaagaaggtaacaattgcttttaaaaattgggttaaacaggccacagaagtttacagacagtttggatctttgatgtg  
 CAGAAGACAATATAAAAGCAAGTTGTCTCTGAAGAAGGTACAATTGCTTTTAAAAATTGGGTAAAAACAGGCACAGAAGTTTACAGACAGTTTGGATCTTTGATGTG  
 gtgcaaaatccacaggaagtgtgatgaacagcagcaacattcaagtttaagcaaaagggtccttatacgtacagagttcgttttctagccaagggaaaatgtaaccag  
 icagttttagggtccttcaactactactgtcgtcgttgaagttcaattcgtttctccaggaatagcatgtctcaagcaaaagatcggttctcttcaattgggtc  
 70 75 80 85 90 95 100 105  
 Val Gln Asn Pro Gln Glu Val Met Met Asn Ser Ser Asn Ile Gln Val Lys Gln Arg Gly Pro Tyr Thr Tyr Arg Val Arg Phe Leu Ala Lys Glu Asn Val Thr Gln

601

gtgcaaaatccacaggaagtgtgatgaacagcagcaacattcaagtttaagcaaaagggtccttatacgtacagagttcgttttctagccaagggaaaatgtaaccag  
 GTGCAAAATCCACAGGAAGTGTGATGAACAGCAGCAACATTCAAGTTAAGCAAAAGGTCCTTATACGTACAGAGTTCGTTTTCTAGCCAAGGAAAATGTAACCCAG  
 :caggacgctgaggacaacacagtcctcttctcgcagcccaatggtgccatcttgaaccttcaactatcagttggaacagaggctgacaacttcaagttctcaactctg  
 jgctctgcaactcctgttctgtcagagaaggagcgtgggttaccaggtagaagcttggaaagtgaatgtaacacttctcagctgttgaaggtcgaaggttagac  
 105 110 115 120 125 130 135 140  
 Gln Asp Ala Glu Asp Asn Thr Val Ser Phe Leu Gln Pro Asn Gly Ala Ile Phe Glu Pro Ser Leu Ser Val Gly Thr Glu Ala Asp Asn Phe Thr Val Leu Asn Leu

602

:caggacgctgaggacaacacagtcctcttctcgcagcccaatggtgccatcttgaaccttcaactatcagttggaacagaggctgacaacttcaagttctcaactctg  
 CAGGACGCTGAGGACAACACAGTCCTCTTCTCGCAGCCCAATGGTGCCATCTTGAACCTTCACTATCAGTTGGAACAGAGGCTGACAACCTCACAGTTCTCAACTCTG  
 ctggctgtggcagctgcatcccatatctatacaaatcaatttgggtcgaatgatcctcaattcaactattatacaagtcgcaaatcttctatgttccaagtcagaactttg  
 gaccgacaccctcgacgtagggtatagatagttttagttaaacaagtttactaggagtttaagtgaaatattgttcagttttagaagatacaaggttcagctctgaaac  
 140 145 150 155 160 165 170 175  
 Leu Ala Val Ala Ala Ala Ser His Ile Tyr Gln Asn Gln Phe Val Gln Met Ile Leu Asn Ser Leu Ile Asn Lys Ser Lys Ser Ser Met Phe Gln Val Arg Thr Leu

603

ctggctgtggcagctgcatcccatatctatacaaatcaatttgggtcgaatgatcctcaattcaactattatacaagtcgcaaatcttctatgttccaagtcagaactttg  
 CTGGCTGTGGCAGCTGCATCCCATATCTATCAAAATCAATTGTTCAAATGATCCTCAATTCACTTATTAACAAGTCAAAATCTTCTATGTTCCAAGTCAGAACTTTG  
 ttgagagaactgttatgggctatagggatccattttgagtttgggtccgtaccctgttactaccacagttggctgttttatccttacaacaatactgcagatgga  
 aactccttgacaatacccgatccctaggtaaaaactcaaaccaaggcatgggcaaatgatggtgcaaccagacaaaataggaatgttattatgagctctaccc  
 175 180 185 190 195 200 205 210  
 Leu Arg Glu Leu Leu Trp Gly Tyr Arg Asp Pro Phe Leu Ser Leu Val Pro Tyr Pro Val Thr Thr Val Gly Leu Phe Tyr Pro Tyr Asn Asn Thr Ala Asp Gly

604

ttgagagaactgttatgggctatagggatccattttgagtttgggtccgtaccctgttactaccacagttggctgttttatccttacaacaatactgcagatgga  
 TTGAGAGAACTGTTATGGGCTATAGGGATCCATTTTGAAGTTGGTCCGTACCCTGTTACTACCACAGTTGGCTGTTTTATCCTTACAACAATACTGCAGATGGA  
 170 360 350 340 330 320 310 300 290 280 270

605

jgagttataaagtttccaatggaaaagataacataaagtaagtgccataatcgacacataaaaggtaaaaggaatctgtcctattgggaaagtcactgacatg  
 cctcaaatattccaaaagtacctttctattgtattcattcaacggatagctgtgtatattccattttccttagacaggataaaccttcagtacgctgtac  
 210 Gly Val Tyr Lys Val Phe Asn Gly Lys Asp Asn Ile Ser Lys Val Ala Ile Ile Asp Thr Tyr Lys Gly Lys Arg Asn Leu Ser Tyr Trp 240 Glu Ser His Cys Asp Met  
 215 220 225 230 235 240 245  
 Cd36 →

606

jgagttataaagtttccaatggaaaagataacataaagtaagtgccataatcgacacataaaaggtaaaaggaatctgtcctattgggaaagtcactgacatg  
 SGAGTTTATAAAGTTTCCAATGGAAAAGATAACATAAAGTAAAGTTGCCATAATCGACACATAAAAGGTAAAAGGAATCTGTCTATTGGGAAAGTCACTGCGCATG.  

  
 atgattaatggtacagatgcagcctcatttccacctttgttgagaaaagccaggattgcagttctttcttctgatattgcaggtcaactctatgctgtattgaa  
 jtactaataccatgtctacgtcggagtaaggtggaaaacaactcttctgggtccataacgtcaagaaaagaagcattaaacgtccagttagatagacataaactt  
 245 Met Ile Asn Gly Thr Asp Ala Ala Ser Phe Pro Phe Val Glu Lys Ser Gln Val Leu Gln Phe Phe Ser Ser Asp Ile Cys Arg Ser Ile Tyr Ala Val Phe Glu  
 250 255 260 265 270 275 280  
 Cd36 →

atgattaatggtacagatgcagcctcatttccacctttgttgagaaaagccaggattgcagttctttcttctgatattgcaggtcaactctatgctgtattgaa  
 ATGATTAATGGTACAGATGCAGCCTCATTTCACCTTTTGTGAGAAAAGCCAGGATTGCAGTCTTTTCTTCTGATATTGCAGGTCAACTCTATGCTGTATTGAA  

  
 160 150 140 130 120 110 100 90 80 70 60

607

tgaatccgacgttaactctgaaggaatccctgtgtatagattgttcttccatccaagcccttgcctcaccagtgaaaaccagacaaactattgttctgcacagaa  
 acttaggctgcaatagacttcttagggacacatctaaacaagaaggtaggttccgaaacggagaggtcaactttgggtctgtgatacaaaagcaggtctctt  
 280 Glu Ser Asp Val Asn Leu Lys Gly Ile Pro Val Tyr Arg Phe Val Leu Pro Ser Lys Ala Phe Ala Ser Pro Val Glu Asn Pro Asp Asn Tyr Cys Phe Cys Thr Glu  
 285 290 295 300 305 310 315  
 Cd36 →

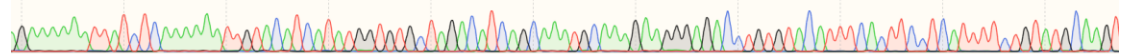
608

tgaatccgacgttaactctgaaggaatccctgtgtatagattgttcttccatccaagcccttgcctcaccagtgaaaaccagacaaactattgttctgcacagaa  
 TGAATCCGACGTTAATCTGAAAGGAATCCCTGTGTATAGATTGTTCTTCCATCCAAGCCCTTGCCTCTCCAGTTGAAAACCCAGACAACTATTGTTCTGCACAGA  

  
 680 670 660 650 640 630 620 610 600 590 580

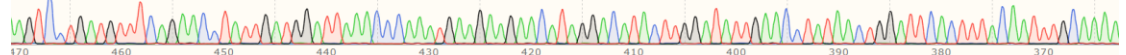
agaaaaaattatctcaaaaaattgtacatcatatgggtgtctagacatcagcaaatgcaagaaggagacctgtgtacatttcaacttctcattttctgtatgcaagt  
 tctttttaaagagtttttaacatgtatgataccacacagatctgtagtcttcttcttctcctcctggacacatgtaaagtgaaggagtaaaagacatcagttca  
 315 Glu Lys Ile Ile Ser Lys Asn Cys Thr Ser Tyr Gly Val Leu Asp Ile Ser Lys Cys Lys Glu Gly Arg Pro Val Tyr Ile Ser Leu Pro His Phe Leu Tyr Ala Ser  
 320 325 330 335 340 345 350  
 Cd36 →

609

agaaaaaattatctcaaaaaattgtacatcatatgggtgtctagacatcagcaaatgcaagaaggagacctgtgtacatttcaacttctcattttctgtatgcaagt  
 AGAAAAAATTATCTCAAAAAATTGTACATCATATGGTGTCTAGACATCAGCAAAATGCAAGAAGGAGACCTGTGTACATTTCACTTCTCATTTTCTGTATGCAAGT  

  
 570 560 550 540 530 520 510 500 490 480 470

iagtcctgatgttcagaacctattgatggattaaacccaatgaagaagaacataggacatacttggatattgaacctataactggattcactttacaattgcaaaa  
 tcaggactacaagctctggataaacctcaatttgggtttacttcttcttctgtatctctgtatgaacctataacttggatattgacctaaagtgaattgttaacgtttt  
 350 Ser Pro Asp Val Ser Glu Pro Ile Asp Gly Leu Asn Pro Asn Glu Glu Glu His Arg Thr Tyr Leu Asp Ile Glu Pro Ile Thr Gly Phe Thr Leu Gln Phe Ala Lys  
 355 360 365 370 375 380 385  
 Cd36 →

610

iagtcctgatgttcagaacctattgatggattaaacccaatgaagaagaacataggacatacttggatattgaacctataactggattcactttacaattgcaaaa  
 IAGTCTGTGATGTTTCAGAACCTATTGATGGATTAACCCAAATGAAGAAGAACATAGGACATACTTGGATATTGAACCTATAACTGGATTCACTTTACAATTTGCAAAA  

  
 470 460 450 440 430 420 410 400 390 380 370

aaacggctgcagggtcaacctattgggtcaagccatcagaaaaaattcaagattaaagaatctgaagaggaactatattgtgcctattctttggcttaatgagactggg  
 ttgcccagctccagttggataaccagttcggtagtcttttaagtccataattcttagactctccttgatataacacggataagaaaccgaattactctgacc  
 385 390 395 400 405 410 415 420  
 Lys Arg Leu Gln Val Asn Leu Leu Val Lys Pro Ser Glu Lys Ile Gln Val Leu Lys Asn Leu Lys Arg Asn Tyr Ile Val Pro Ile Leu Trp Leu Asn Glu Thr Gly  
 Cd36 →

aaacggctgcagggtcaacctattgggtcaagccatcagaaaaaattcaagattaaagaatctgaagaggaactatattgtgcctattctttggcttaatgagactggg  
 AAACGGCTGCAGGTC AACCTATTGGTCAAGCCATCAGAAAAAATTC AAGATTAAAGAATCTGAAGAGGAAC TATATTGTGCCTATTCTTTGGCTTAATGAGACTGGG.  
 360 350 340 330 320 310 300 290 280 270 260

611

gggaccattgggtgatgagaaggcaaacatggtcagaagtcaagtaactggaaaaataaacctcctggcatggtagagatggccttacttgggattggagtggtgat  
 cccctggtaaccactactctccggttgtaacaagcttcagttcatgaccttttatttggaggaaccgtaccatctaccggaatgaaccctaacctcaccactac  
 420 425 430 435 440 445 450 455  
 Gly Thr Ile Gly Asp Glu Lys Ala Asn Met Phe Arg Ser Gln Val Thr Gly Lys Ile Asn Leu Leu Gly Met Val Glu Met Ala Leu Leu Gly Ile Gly Val Val Met  
 Cd36 →

gggaccattgggtgatgagaaggcaaacatggtcagaagtcaagtaactggaaaaataaacctcctggcatggtagagatggccttacttgggattggagtggtgat  
 GGGACCATTGGTGATGAGAAGGCAAACATG GTCAGAAGTCAAGTAACTGGAAAAATAAACCTCCTGGCATGGTAGAGATGGCCTTACTTGGGATTGGAGTGGTGATC  
 160 250 240 230 220 210 200 190 180 170 160

612

gatgtttgtgcttttatgatttcatttggcttgcaaatccaagaatggaaaaataagtagtggatgagcctacatatacactggctacatcttggtaaaagccgat  
 ctacaacaacgaaaatacctaaagtataacacgaacggttaggttcttacctttatctcatcacctactcggatgtatattgaccgatgtagaaaccatttcgctat  
 455 460 465 470  
 Met Phe Val Ala Phe Met Ile Ser Tyr Cys Ala Cys Lys Ser Lys Asn Gly Lys  
 Cd36 → exon  
 Met Phe Val Ala Phe Met Ile Ser Tyr Cys Ala Cys Lys Ser Lys Asn Gly Lys  
 (in frame with CD36)

gatgtttgtgcttttatgatttcatttggcttgcaaatccaagaatggaaaaataagtagtggatgagcctacatatacactggctacatcttggtaaaagccgat  
 GATGTTTGTGCTTTTATGATTTCATTTGCTTGCAAATCCAAGAATGGAAAAATAAGTAGTGGATGAGCCTACATATACACTGGCTACATCTTGGTAAAGCCGAT  
 150 140 130 120 110 100 90 80 70 60 50

613

614 S5 Fig. The full-length Sanger sequencing data of the CD36 CDS in homozygous

615 hCD36 mice.

616

617